Simplified Numerical Electromagnetic Field Analysis Method of Coils Wound with Spiral Coated-Conductor Cables

Yusuke Sogabe, *Member*, *IEEE*, Rikito Takahashi, and Naoyuki Amemiya, *Member*, *IEEE*

***Abstract*—To reduce the computation load for electromagnetic field analyses of magnets wound with spiral coated-conductor cables, we developed a simplified analysis method. In the method, we analyze a single spiral coated-conductor cable carrying transport current under the external magnetic field, which is generated by the current in adjacent spiral coated-conductor cables while ignoring influence of shielding currents in them. We conducted numerical electromagnetic field analyses with and without the model and directly compared the analysis results: magnetization and ac loss density distributions in coated conductors and the temporal evolution of ac losses. The comparison of the analysis results from each analysis model showed the applicability of the analysis method for ac loss estimation of magnets.**

***Index Terms*—AC loss, conductor on round core cable, electromagnetic field analysis, high-T_c superconducting coil, simplified analysis method, spiral coated-conductor cable.**

I. Introduction

A spiral coated-conductor cable is shown in Fig. 1. It is a cable comprising several coated conductors wound in a spiral around a round core. A conductor on round core (CORC®) cable is a type of spiral coated-conductor cables. The spiral coated-conductor cable has a circular cross-section, that allows for a high degree of freedom with respect to bending when it is wound into a coil. Owing to their mechanical strength and large current capacity, spiral coated-conductor cables are expected to be used for coil winding of superconducting magnets [1-6].

The estimation of ac losses in high-T_c superconducting (HTS) coil windings is quite important to discuss their applicability to ac machines, such as stator coils in rotating machines, or ac magnets, such as magnets for synchrotrons. This is also the case for coils wound with spiral coated-conductor cables. Numerical electromagnetic field analysis is a powerful tool to estimate the ac losses of HTS cables and coils. Some studies have been conducted to evaluate the characteristics of various spiral coated-conductor cables by performing numerical electromagnetic field analyses [7-9]. However, strict numerical electromagnetic field analyses of coils wound with spiral coated-conductor cables are not realistic owing to the huge analysis costs caused by the three-dimensional geometry of the coated conductors in the cables and the small pitch length compared with the total length of the cables wound into coils. Therefore, we need to develop a simplified numerical electromagnetic field analysis method with an appropriate model of magnets wound with spiral coated-conductor cables. Although there have been several previous studies on the simplification of the numerical electromagnetic field analysis of ac losses and shielding currents in coils wound with single coated conductors [10-12], there have been few studies on the simplification method of numerical electromagnetic field analysis of magnets wound with spiral coated-conductor cables.

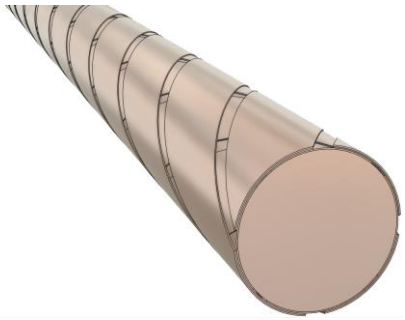

Fig. 1. Schematic of a spiral coated-conductor cable. The cable composed of six coated conductors (two coated conductor per layer and three layer) and a round core.

In this paper, we report a simplified numerical electromagnetic field analysis method for coils wound with spiral coated-conductor cables. The proposed method analyzes a single straight spiral coated conductor, which corresponds to one turn of the analyzed coil, exposed to a magnetic field in the coil cross-section [13]. In the analysis method, as shielding currents in adjacent spiral coated-conductor cables are ignored, the calculated ac loss in the spiral coated-conductor cable could include errors. We constructed analysis models with and without the analysis method and compared the analyzed ac losses.

This work was supported in part by JSPS KAKENHI Grant Number JP20H00245, in part by JST-Mirai Program Grant Number JPMJMI19E1, Japan , and in part by Japan-U.S. Science and Technology Cooperation Program in High Energy Physics. *(Corresponding author: Naoyuki Amemiya.)*

The authors are with the Department of Electrical Engineering, Kyoto University, Kyoto 615-8510, Japan (e-mail: amemiya.naoyuki.6a@kyoto-u.ac.jp).

Color versions of one or more of the figures in this paper are available online at http://ieeexplore.ieee.org.

Digital Object Identifier will be inserted here upon acceptance.

II. Simplified Numerical Electromagnetic Field Analysis Method

A. Simplification of Shielding Current Calculation

We proposed a simplified electromagnetic model of magnets wound with spiral coated-conductor cables for ac loss calculations [13]. In the modeling, a single spiral coated-conductor cable corresponding to the turn of an analyzed coil is analyzed considering the three-dimensional structure of the coated conductors composing the cable. For the analysis of one single spiral coated-conductor cable, we used the three-dimensional model of the cable to consider the influence of its three-dimensional structure, instead of the two-dimensional cross-sectional model of the cable. The analyzed cable is exposed to a magnetic field that is calculated with the assumption that currents are distributed uniformly in the coated conductors composing the adjacent cables. Here, we ignored the shielding currents in adjacent cables, namely, the interactions among the shielding currents in the analyzed cable and those in the adjacent cables are not considered in the electromagnetic field analysis for ac loss calculation.

By applying the simplification to the ac loss analyses, we could drastically reduce calculation costs, such as calculation time and memory consumption. However, the validity of this simplification have not been discussed.

B. Analysis Models for Validation of Simplified Method

To directly compare the analysis results of the models with and without the simplified method, we developed the following three models, and their schematics are shown in Fig. 2.

1) Nine cables arranged in three horizontal and three vertical rows were analyzed. This model represents the analysis model without a simplified method, which is the most rigorous analysis model possible.
2) One of the nine cables was analyzed, and the influence of shielding currents induced in other cables was ignored. Forced currents uniformly distributed in the coated conductors of the non-analyzed cables are considered sources of an external magnetic field to the analyzed cable, and three-dimensional geometry of the non-analyzed cables is considered.
3) A single cable was analyzed. This model is a reference for the ac loss calculation.

The analyses were conducted under the condition that the same temporal profile of ac current and ac magnetic field was applied to each model. We compared the ac loss distribution and the time variation of the ac loss. However, when calculating the ac loss generated in all nine cables from the analysis results of model 2, the analysis was separately performed for nine cables, and the ac loss calculated for each cable was added together to estimate the ac loss. On the contrary, for model 3, the calculated ac loss values were multiplied by nine to estimate the ac loss generated for all nine cables.

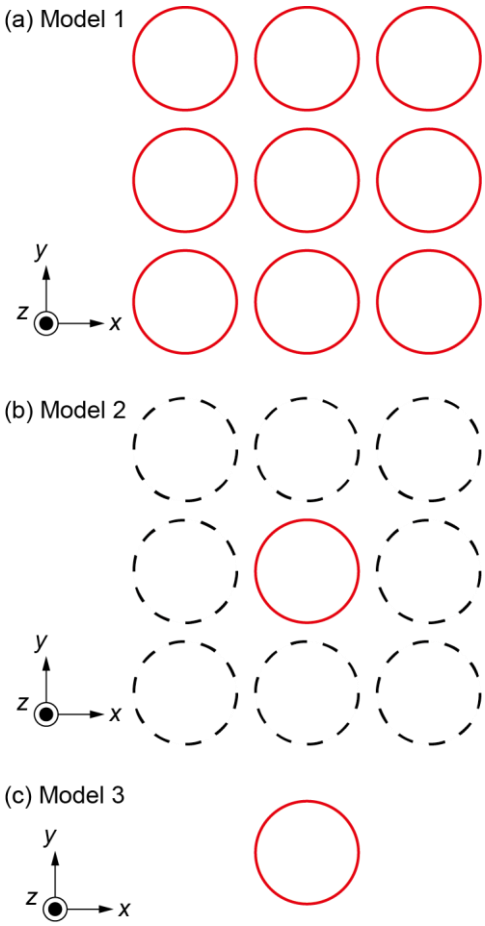

Fig. 2. Cross-sectional schematics of analysis models used in the study: (a) model 1, (b) model 2, and (c) model 3. Red circles with solid lines represent the analyzed spiral coated-conductor cables (in the cables, shielding currents are calculated). Black circles with broken lines represents the non-analyzed spiral coated-conductor cables (in the cables, shielding currents are not calculated, but forced currents are considered as sources of external fields to analyzed cables). In Fig. 2(b), the center cable is an analyzed cable as an example.

C. Numerical Electromagnetic Field Analysis for AC Loss Calculation

For ac loss calculations of spiral coated-conductor cables, we used the finite element method with the *T*-formulation and thin-strip approximation [14]. The equation to be solved in the analyses is derived from Faraday's law, Biot–Savart's law, Ohm's law, and the definition of the current vector potential *T* as follows:

$$\nabla\times\left(\frac{1}{\sigma}\nabla\times\boldsymbol{n}T\right)\cdot\boldsymbol{n}+\frac{\partial}{\partial t}\frac{\mu_0 t_s}{4\pi}\cdot\left(\int_{S'}\left[\left\{\left(\nabla\times\boldsymbol{n}'T'\right)\times\boldsymbol{r}\cdot\boldsymbol{n}\right\}/r^3\right]\mathrm{d}S'+\boldsymbol{B}_{\mathrm{ext}}\cdot\boldsymbol{n}\right)=0. \tag{1}$$

Here, T and T' denote the magnitudes of the current vector potentials at the field point where the potential is calculated and the source point where the current exists, respectively. $\boldsymbol{n}$ and $\boldsymbol{n}'$ are normal vectors at the field point and source points, respectively, and $\boldsymbol{r}$ is a vector from the source point to the field point. t_s and σ denote the thickness of the superconductor lay-

TABLE I
PARAMETERS OF ANALYZED SPIRAL COATED-CONDUCTOR CABLES

Number of layers	3	Pitch length	5.6 mm
Number of coated conductors per layer	2	Core diameter	2.5 mm
Width of coated conductor	2 mm	Thickness of coated conductor	45 μm
Thickness of superconductor layer	1.75 μm	Separation between cables[a]	0.6 mm

[a]This is only applied to models 1 and 2.

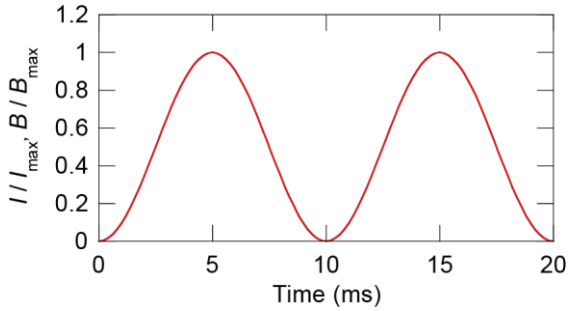

Fig. 3. Temporal profile of current per coated conductor I and externally applied magnetic flux density B. Here, I and B are normalized by maximum current per coated conductor I_{max} and maximum externally applied magnetic flux density B_{max}, respectively.

er and its equivalent conductivity, respectively. $\boldsymbol{B}_{ext}$ is the external magnetic flux density. S' is the area of the wide face of the superconductor layer of the coated conductors.

Spiral coated-conductor cables have a short spiral pitch: it is a few millimeters in practical CORC® cables [1]. In this situation, a very fine mesh structure is required to conduct precise analyses of multiple spiral coated-conductor cables. To handle analyses with many degrees of freedom, we applied hierarchical matrices [14] that can drastically reduce calculation time and memory consumption.

Moreover, although an infinitely long cable model is sometimes used to analyze cables composed of coated conductors, such as Roebel cables or CORC® cables, using the assumption that the cables have translational symmetry in the cable direction, ill-conditioned matrices can appear in analyses of the cables under the assumption of translational symmetry, and the convergence of the analyses can be worse than analyses without translational symmetry. Therefore, we developed a finite-long model of spiral coated-conductor cables.

III. Analyzed Spiral Coated-Conductor Cables and Analysis Conditions

The parameters of the analyzed spiral coated-conductor cables are listed in Table I. A bird view schematic of the analyzed spiral coated-conductor cable is shown in Fig. 1. The parameters of the cable in the analyses were defined based on an actual CORC® wire. In addition, we analyzed three pitches for each cable. In the ac loss calculations, each half pitch at both ends was not used because of the strong influence of the ends of the cables, and only the two pitches in the center part were used.

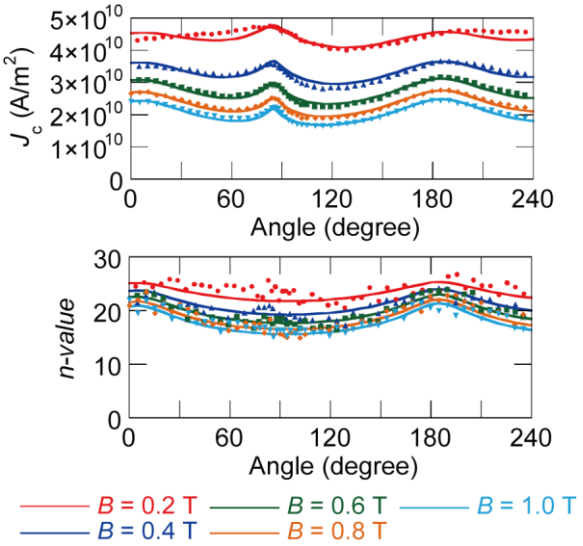

Fig. 4. Dependence of measured and formulated EJ characteristics on magnetic field. Measured critical current density J_c and n-value are plotted with dots, and formulated them are plotted with lines.

The temporal evolution of the transport current and external magnetic field is shown in Fig. 3. I is the current per coated conductor, and it is assumed that the same current flows in all coated conductors that make up the cable. Here, I_{max} is set at 30 A, B_{max} is set at 0.8 T and its direction is the same as the y-axis shown in Fig. 2. The frequency of the current and external magnetic fields is 100 Hz [13].

In the analyses, we used the electric field E–current density J characteristics of an actual coated conductor manufactured by SuperPower Inc. at 65 K. To formulate the E–J characteristics, we used a power-law model considering the dependence of the critical current density J_c and n-value on the magnitude and angle of the magnetic field B and ϕ described in [15]. The measured and formulated J_c and n-value are shown in Fig. 4.

IV. Analysis Results and Discussions

A. Magnetization and AC Loss Density Distributions

Ignoring the shielding current in adjacent spiral coated-conductor cables may affect the electromagnetic field distribution in the coated conductors that make up the cables. As the calculated ac losses in the cable differ under different electromagnetic field distributions, the magnetization and ac loss density distributions in the cable are compared before investigating the influence of model differences on the ac losses.

The magnitude of the magnetization $\mu_0 M$ distribution at t = 12 ms in a cable is shown in Fig. 5. The center cables of the nine cables in a 3 × 3 arrangement are shown in Figs. 5(a) and 5(b). The region enclosed by the red broken line is where the wide surface of the coated conductor in the outermost layer of the spiral coated-conductor cable is perpendicular to the applied magnetic field, and where the magnetization is the largest. The red broken area shows that the magnetization of the coated conductor calculated by the analysis using model 1 is larger than that calculated by the analysis using model 2. This is caused by the shielding currents in the adjacent cable that

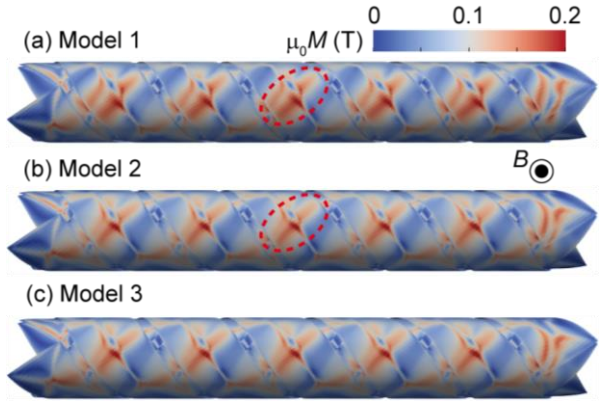

Fig. 5. Magnetization $\mu_0 M$ distribution at t = 12 ms in the spiral coated-conductor cable calculated by (a) model 1, (b) model 2, and (c) model 3. For models 1 and 2, the center cable of the nine cables in a 3 × 3 arrangement is shown in the figure.

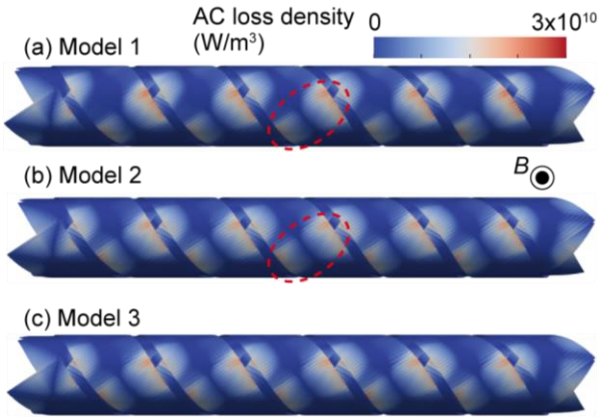

Fig. 6. AC loss density distribution at t = 12 ms in the spiral coated-conductor cable calculated by (a) model 1, (b) model 2, and (c) model 3. For models 1 and 2, the center cable of the nine cables is in a 3 × 3 arrangement.

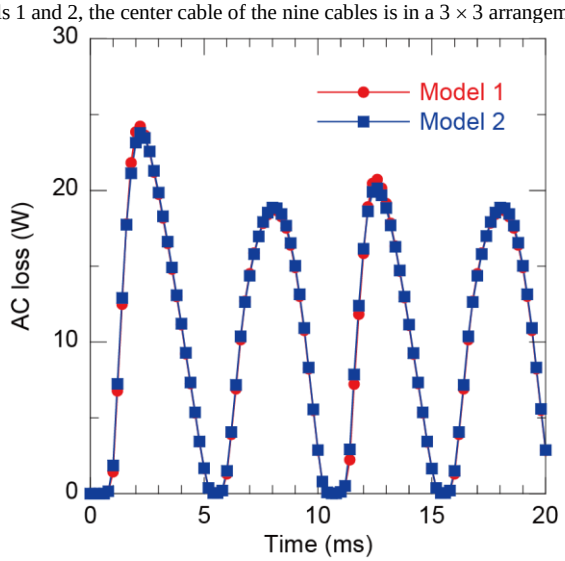

Fig. 7. Temporal evolution of ac losses in the nine cables calculated by models 1 and 2.

shielded the external magnetic field to the center cable. As a result, the magnetization distribution, that is, the shielding current distribution, in the analyzed cable was different depending on whether the shielding current calculation was simplified. Meanwhile, there was no difference in the magnetization distributions calculated using models 2 and 3. This indicates that the magnetic field generated by the forced current of the adjacent cables has little influence on the magnetic field distribution at the central cable.

Fig. 6 shows the ac loss density distributions at t = 12 ms in the cable calculated by the models 1, 2, and 3. The center cables of the nine cables in a 3 × 3 arrangement are shown in Figs. 6(a) and 6(b). In contrast to the magnetization distribution, there was no significant difference in the calculation results from models 1 and 2. The point of large magnetization locates in the middle of the shielding current loop, and the current density at that point is low. On the contrary, Figs. 5 and 6 show that the points with high current density, where the ac loss density becomes high, are located at both ends in the width direction of the point with large magnetization. In other words, the difference in the magnitude of magnetization itself does not have a considerable influence on the ac loss density distribution. Furthermore, the ac loss density distribution calculated by model 3 agrees with that calculated by models 1 and 2.

The point to be considered in applying simplification method is the distance between cables. The shielding current in adjacent cables, namely the effect of magnetization in adjacent cables on the magnetic field distribution at other cable locations, is considered to be inversely proportional to the square of the distance between cables. If the cables are close enough to contact each other, it may not be reasonable to calculate the ac loss by ignoring the interaction of shielding currents in each cable.

B. Temporal Evolution of AC Losses

While the previous subsection focused on the electromagnetic field distribution in the cable at a single time, this subsection discusses the temporal evolution of the ac loss. Fig. 7 shows the temporal evolution of the ac losses calculated using models 1 and 2. During the ramp-up phase of the current and external magnetic field, there was some difference between the calculated ac losses by models 1 and 2, but the relative difference was approximately 15% even at the largest time (t = 11 ms). Moreover, as ac losses at the time are relatively small, their difference does not have a considerable influence on the calculated total ac losses for the cycle. When the ac losses of the second cycle were integrated and compared, the relative error between models 1 and 2 was approximately 1.7%. Although not shown in Fig. 7, as expected from the discussion so far, models 2 and 3 agree with sufficient accuracy, and the relative error between them is approximately 0.2%. The ac loss density distribution in each cable in model 2 was almost identical because the externally applied magnetic field was sufficiently larger than the magnetic field generated by the transport current flowing the 3 × 3 aligned cables. Therefore, the ac losses in models 2 and 3 were almost identical with a relative error of 0.2%.

This accuracy is sufficient from the viewpoint of predicting ac loss by numerical electromagnetic field analysis, and analysis using models 2 or 3, that is, simplification of shielding current calculation, is a reasonable method for ac loss calculation.

For coils with a large number of turns, model 3 is considered to be sufficient for ac loss evaluation. However, if the number of turns in the coil is small and the magnetic field distribution in the cross-section of the spiral cable cannot be regarded as uniform, model 2 is considered to be more appropriate for ac loss estimation.

In model 3, it is not actually necessary to conduct the analyses for all turns, since the ac losses in the spiral coated-conductor cables at different locations in the magnet will be the same if the amplitude of the externally applied magnetic field is the same. In terms of computational costs, model 3 can calculate the ac loss with about 1/80 of the memory consumption and computation time of model 1 under the present analysis conditions. In addition, the time required to evaluate the ac loss across the magnet is even shorter than in model 1, because the analyses with model 3 can be conducted for cables at several different locations in parallel.

V. Conclusion

A coil composed of spiral coated-conductor cables was analyzed, and the effect of simplifying the shielding current calculation in adjacent cables on the analysis accuracy was evaluated by analyses. The comparison of the calculated ac losses from the analyses with and without the simplification showed the applicability of the analysis model using the simplified model for ac loss evaluation of coils. This result suggests that evaluating the ac loss characteristics of the coil by repeating the analysis of a single spiral coated-conductor cable several times is possible, thereby facilitating the ac loss evaluation of coils composed of spiral coated-conductor cables.

References

[1] D. C. van der Laan, J. D. Weiss, P. Noyes, U. P. Trociewitz, A. Godeke, D. Abraimov, and D. C. Larbalestier, “Record current density of 344 A mm^{-2} at 4.2 K and 17 T in CORC® accelerator magnet cables,” *Supercond. Sci. Technol.*, vol. 29, no. 5, Apr. 2016, Art. no. 055009.

[2] X. Wang, S. Caspi, D. R. Dietderich, W. B. Ghiorso, S. A. Gourlay, H. C. Higley, A. Lin, S. O. Prestemon, D. van der Laan, and J. D. Weiss, “A viable dipole magnet concept with REBCO CORC® wires and further development needs for high-field magnet applications,” *Supercond. Sci. Technol.*, vol. 31, no. 4, Mar. 2018, Art. no. 045007.

[3] M. Vojenčiak, A. Kario, B. Ringsdorf, R. Nast, D. C. van der Laan, J. Scheiter, A. Jung, B. Runtsch, F. Gömöry, and W. Goldacker, “Magnetization ac loss reduction in HTS CORC® cables made of striated coated conductors,” *Supercond. Sci. Technol.*, vol. 28, no. 10, Sep. 2015, Art. no. 104006.

[4] P. C. Michael, L. Bromberg, D. C. van der Laan, P. Noyes, and H. W. Weijers, “Behavior of a high-temperature superconducting conductor on a round core cable at current ramp rates as high as 67.8 kA s^{-1} in background fields up to 19 T,” *Supercond. Sci. Technol.*, vol. 29, no. 4, Feb. 2016, Art. no. 045003.

[5] T. Mulder, A. Dudarev, M. Mentink, H. Silva, D. van der Laan, M. Dhallé, and H. ten Kate, “Design and Manufacturing of a 45 kA at 10 T REBCO-CORC Cable-in-Conduit Conductor for Large-Scale Magnets,” *IEEE Trans. Appl. Supercond.*, vol. 26, no. 4, Jun. 2016, Art. no. 4803605.

[6] C. S. Myers, M. D. Sumption, and E. W. Collings, “Magnetization and Flux Penetration of YBCO CORC Cable Segments at the Injection Fields of Accelerator Magnets,” *IEEE Trans. Appl. Supercond.*, vol. 29, no. 5, Aug. 2019, Art. no. 4701105.

[7] Y. Sogabe, Y. Mizobata, and N. Amemiya, “Coupling time constants and ac loss characteristics of spiral copper-plated striated coated-conductor cables (SCSC cables),” *Supercond. Sci. Technol.*, vol. 33, No. 5, Apr. 2020, Art no. 055008.

[8] J. Sheng, M. Vojenčiak, R. Terzioğlu, L. Frolek and F. Gömöry, "Numerical Study on Magnetization Characteristics of Superconducting Conductor on Round Core Cables," *IEEE Trans. Appl. Supercond.*, vol. 27, no. 4, Jun. 2017, Art no. 4800305.

[9] B. Shen et al., "A Simplified Model of the Field Dependence for HTS Conductor on Round Core (CORC) Cables," *IEEE Trans. Appl. Supercond.*, vol. 31, no. 8, Nov. 2021, Art no. 4803405.

[10] Y. Sogabe, T. Tsukamoto, T. Mifune, T. Nakamura, and N. Amemiya, “Efficient and practical models for numerical electromagnetic field analyses of three-dimensional-shape coils wound with coated conductor,” *IEEE Trans. Appl. Supercond.*, vol. 25, no. 3, Jun. 2015, Art no. 4900205.

[11] V.M.R. Zermeño and F. Grill, “3D modeling and simulation of 2G HTS stacks and coils,” *Supercond. Sci. Technol.*, vol. 27, No. 4, Mar. 2014, Art no. 044025.

[12] S. Noguchi, T. Imai, D. Park, S. Hahn, and Y. Iwasa, “A simple screening current simulation method using equivalent circuit model for REBCO pancake coils,” *Supercond. Sci. Technol.*, vol. 33, No. 11, Sep. 2020, Art no. 115005.

[13] Y. Sogabe, M. Yasunaga and N. Amemiya, "Simplified Electromagnetic Modelling of Accelerator Magnets Wound With Conductor on Round Core Wires for AC Loss Calculations," *IEEE Trans. Appl. Supercond.*, vol. 30, no. 4, Jun. 2020, Art no. 4004005.

[14] T. Mifune, N. Tominaga, Y. Sogabe, Y. Mizobata, M. Yasunaga, A. Ida, T. Iwashita, and N. Amemiya, “Large-scale electromagnetic field analyses of coils wound with coated conductors using a current-vector-potential formulation with a thin-strip approximation,” *Supercond. Sci. Technol.*, vol. 32, no. 9, Jul. 2016, Art. no. 094002.

[15] Y. Sogabe, Z. Jiang, S. C. Wimbush, N. M. Strickland, M. Staines, N. J. Long, and N. Amemiya, “AC loss characteristics in REBCO coil assemblies with different geometries and conductors,” *IEEE Trans. Appl. Supercond.*, vol. 28, no. 3, Apr. 2018, Art no. 4700105.